



Original Research

Lung Chest X-Ray Image Segmentation for Detection of Pneumonia using Convolutional Neural Network

Nur Amyza Arjuna¹, Asnida Abdul Wahab^{1,2*}, Gan Hong Seng³, Maheza Irna Mohamad Salim¹, Muhammad Hanif Ramlee¹

¹ School of Biomedical Engineering and Health Sciences, Faculty of Engineering, Universiti Teknologi Malaysia, Skudai 81310, Johor, Malaysia

² Medical Device and Technology Center (MEDITEC), Universiti Teknologi Malaysia, Skudai 81310, Johor, Malaysia

³ Department of Data Science, Universiti Malaysia Kelantan, 16100 UMK City Campus Pengkalan Chepa, Kelantan, Malaysia

ARTICLE INFO

Article History:

Received 17 August 2022

Accepted 5 September 2022

Available online 15 September 2022

Keywords:

Lung segmentation,

Chest x-ray,

Convolutional Neural Network.

ABSTRACT

Pneumonia has been identified as the top cause of mortality in children under the age of five, as well as in elderly with comorbidities. According to the World Health Organization, pneumonia reported 14% fatalities in children under the age of five nationwide in 2019. Chest x-ray (CXR) has been commonly used for detection of pneumonia. However, factor such as noise with low levels of intensity and low contrast between the images and the boundary representation can modify CXR images and it also requires highly skilled medical practitioners to accurately interpret the CXR images. Therefore, the goal of this study is to develop an automatic segmentation model to segment the region of interest (ROI) of pneumonia lung CXR images using U-Net architecture. Image enhancement using Contrast Limited Adaptive Histogram Equalisation (CLAHE) and gamma-correction based enhancement technique were applied to increase the quality of CXR images. Statistical analysis on features extracted from the segmented lung CXR images was performed to analyze the performance of the model was developed. The U-Net segmentation model achieves 95.58%, 95.82% and 95.48% accuracy for normal CXR while the model achieves 86.76%, 87.98% and 86.21% accuracy for pneumonia CXR which indicate that the U-Net segmentation for CLAHE x-ray images has better performance in segmenting the ROI of the lungs. As a conclusion, the segmentation model proposed shown to be able to overcome the disadvantages of manual segmentation where the model can be used to perform segmentation automatically on many CXRs at a time.

INTRODUCTION

Pneumonia is an acute respiratory disease that affects the lungs' small sacs called alveoli. When a person has pneumonia, the alveoli get clogged with pus and fluid, resulting in symptoms such as coughing, fever, chills, and trouble breathing owing to a lack of oxygen. Pneumonia is the leading infection that affects the human population and causes mortality especially in children. The World Health Organization (2021, November 11) reported that in 2019, pneumonia killed 740 180 children under the age of five, accounting for 14% of all fatalities in children

under the age of five, but 22% of all deaths in children aged one to five nationwide.

One of the most commonly utilized imaging modalities in the identification of pneumonia is chest x-ray (CXR). CXR is preferred due to its non-invasive characteristics, able to identify a wide range of pathology, cost effective, less exposure of radiation to patients, simple and easily available (Mittal et al., 2017). In this respect, CXR is unquestionably a significant diagnostic technique that aids in the identification of a wide range of lung disorders all over the world (Souza et al., 2019). Despite its ease of acquisition, it is also one of the most challenging imaging modalities to comprehend. Its interpretation is heavily reliant on the individual's level of training and experience (Mittal et al., 2017). The lack of critical analysis of information captured in the images of CXR

* Asnida Abdul Wahab,

Medical Device and Technology Center (MEDITEC), Universiti Teknologi Malaysia, Skudai 81310, Johor, Malaysia

contributes to inconsistent outcomes (Teixeira et al., 2021). Thus, a computer-aided diagnosis (CAD) system that can automatically analyse CXR would be desirable to support medical physicians in making decisions and appropriately interpreting results (Mittal et al., 2017). Study by Mazzone et al. (2013) proved that computer-aided diagnosis (CAD) systems are able to identify and distinguish features of lung CXR precisely for certain disorders and minimize the burden of radiologists at the same time enable remote diagnosis. CAD systems have been developed during the last few decades to retrieve useful information from X-rays.

Image segmentation is significantly vital in radiology and radiation oncology. An accurate and reliable segmentation might aid in either better detection of anomalies or more effective disease treatment (Jahangard et al., 2020). Lung segmentation is a key stage in CAD systems for diagnosis of lung disease (Qin et al., 2018). Lung segmentation divides an image into a number of regions based on visual features that are nearly constant in each zone (Crisan & Holban, 2014). It can offer structural information on shape irregularities as well as lung size measurements, which can be used to assess severe clinical disorders such as pleural effusion and pneumothorax (Dallal et al., 2017). The lung segmentation mask correctly identifies the lung area and also defines the non-lung region through exclusion, reducing the influence of imaging artifacts in the CAD system (Wang et al., 2017).

Segmentation in image processing can be performed mainly through manual segmentation and automated segmentation. Manual segmentation entails labelling the 3D structure in each 2D slice thoroughly. Many models have been proposed for manual segmentation. The active contour model notably known as 'snakes' is one of the most successful methods. The active contour model represents the object boundary as a parameter or curve surface. Since the curve surface is associated with the energy function, therefore the detection of the object boundary is cast as an energy minimization process. Typically, the curves are affected by both an internal force and external force. An active contour can locate object contours well, once an appropriate initialization is done (Nirmala Devi & Kumaravel, 2008). However, because the energy minimization is done locally, the contours that are found can be trapped by a local minimum. Therefore, a variety of methods have been proposed to increase the snakes' performance. In order to address the problem, Xu & Prince (1998) proposed a new deformable model called the 'gradient vector flow snake' (GVF). This method implements a spatial diffusion of the gradient of the image's edge map instead of using the image gradients as an external force directly. Other than that, there are also other methods that have been proposed such as edge-based active contour method and region-based active contour method (Lie et al., 2006). The edge-based active contour models utilize image gradients in order to identify object boundaries while region-based active contour utilize the statistical information inside and outside the contour to control the evolution, which are less sensitive to noise. The region-based active contour model is significantly less sensitive to the location of initial contour and can efficiently detect the exterior and interior boundaries simultaneously (Ramudu et al., 2013).

Although manual segmentation is very comprehensive and reliable, it is not practical to be applied on a large scale and it is not extensively used in clinical application. Therefore, the aims of this study are to develop an automated lung segmentation using CXR images for pneumonia detection. In recent years,

there are a lot of studies that propose an automated segmentation framework. Automated CAD system that ensemble Artificial Intelligence (AI) has been developed for image segmentation of chest x-ray images (Mique & Malicdem, 2020). Deep learning technology has achieved good results in medical image analysis with the advancement of computer image processing capabilities and the continuous enrichment of datasets (Qin et al., 2018). Convolutional neural networks (CNNs), which is a subset of deep learning, have been frequently employed in medical diagnostics (Kundu et al., 2021). The advent of deep learning models to automate the segmentation process assists in the delineation of the lung region in order to identify the frequency of abnormalities. CNNs are built with a variety of building blocks, including convolution layers, pooling layers, and fully connected layers, to learn spatial hierarchies of information automatically and adaptively via backpropagation from low- to high-level patterns. The U-Net CNN architecture is a modification of CNN to enhance the resolution of the output. The architecture is modified to complement the conventional CNN with consecutive layers where pooling operators are substituted by upsampling operators. One significant change in the architecture is that it has a large number of feature channels in the upsampling section, which allows the network to pass context information to higher resolution layers.

The expanding path is symmetric to the contracting path and produces a u-shaped structure. There are no fully linked layers in the network and only use the valid portion of each convolution comprises the pixels in the supplied picture for which the entire context is accessible. This method enables an image segmentation algorithm to seamlessly segment arbitrarily big pictures by using the tile-overlap approach.

MATERIALS AND METHOD

Data Acquisition

The database collected comprises a mixture of 10192 normal and 1345 pneumonia chest x-rays (CXR) and was obtained from Kaggle. The database was created by a team of researchers from Qatar University, Doha, Qatar, and the University of Dhaka, Bangladesh along with their collaborators that combines the normal and pneumonia CXR from two different datasets. The normal CXR dataset used was collected from the Radiological Society of North America while the pneumonia CXR dataset used was collected from the Guangzhou Women and Children's Medical Center, Guangzhou. In this dataset, all pneumonia CXR were originally screened for quality control before being analysed where all low quality or unreadable scans being removed. In this database, they also created segmented lung masks dataset to be used as ground truth during the segmentation process. From the images obtained, only 400 images of normal CXR and 495 images of pneumonia CXR were used in this study. Data analysis was performed and the characteristics of the CXR were evaluated based on the area of the white spots of the pneumonia CXR. Only CXR images that have obvious white spots are chosen. Other than that, this study also performed resize and rescaling on the CXRs datasets. The size of the original images downloaded from the database is 384x384. The images were then resized to 128x128, the dimension of images was chosen because it is the most suitable for U-Net segmentation model. The resize was performed for all CXR images and masks of normal and pneumonia.

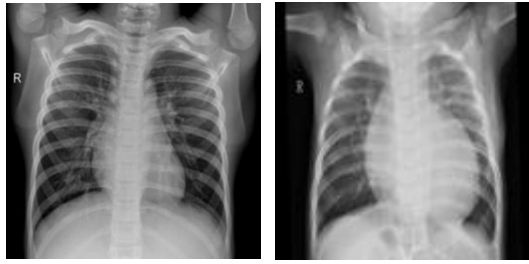


Fig. 1 CXR images sample.

Contrast Enhancement

Image enhancement is an important pre-processing approach in image processing that highlights important information in an image while minimizing or deleting secondary information to improve identification quality. The idea is to make the CXR images more relevant for a certain application than the original images. This study performed a comparative analysis between two different enhancement techniques namely contrast limited adaptive histogram equalization (CLAHE) and gamma correction-based enhancement technique. Both techniques were applied to all CXRs images and then used for segmentation and the performance was evaluated from the segmentation output.

CLAHE is a new contrast enhancement technique has been proposed to overcome drawbacks from adaptive histogram equalization (AHE) method where it can prevent the overamplification of noise that occurs. Since AHE applies histogram equalisation to small bits of the image that enhance the contrast of each region individually, it will adaptively improve local contrast and edges in each area of the picture based on the local distribution of pixel intensities instead of the global information in the image. Therefore, it may overamplify the image's noise component CLAHE employs a contrast amplification limiting method that is performed to each neighbouring pixel and then generates a transformation function to minimize the noise. CLAHE restricts amplification by clipping the histogram at a user-specified value known as clip limit. The clipping level controls how much noise in the histogram is smoothed and hence how much contrast is increase.

The image was divided into multiple non-overlapping areas of almost similar size. The histogram of each area is then computed. The clip limit for clipping histograms is then determined. Next, each histogram is reallocated such that its height does not exceed the clip limit. The clip limit is derived by, which can be expressed as equation (1) (Koonsanit et al., 2017):

$$\beta = \frac{MN}{L} \left(1 + \frac{\alpha}{100} (S_{max} - 1) \right) \tag{1}$$

where β is the clip limit, $M \times N$ is number of pixels in each area, L represents the number of grayscales, α is a clip factor (0- 100), and S_{max} is the maximum allowable slope. From equation (1), if $\alpha=0$, then the clip limit $= \frac{MN}{L}$.

Gamma correction is a non-linear operation performed on the pixels of the source picture. Gamma correction uses the projection link between the value of the pixel and the value of the gamma according to the internal map to enhance the image by alternating the pixel value.

The projection relationship between pixel value and gamma value was established according to the internal map to alternate the pixel value. Equation (2) defined the linear map from P to Ω (Yu et al., 2020; Apostolopoulos & Mpesiana, 2020):

$$\phi: P \rightarrow \Omega, \Omega = \{\omega | \omega = \phi(x)\}, \phi(x) = \frac{\pi x}{2xm} \tag{2}$$

where P represents the pixel value within the range $[0,255]$, Ω represents the angle value, I' is the symbol of the gamma value set, and x is the pixel's grayscale value ($x \in P$), xm is the midpoint of the range $[0, 255]$.

Equation (3) defined the mapping from Ω to I

$$h: \Omega \rightarrow I', I' = \{\gamma | \gamma = h(x)\} \tag{3}$$

$$\begin{cases} h(x) = 1 + f_1(x) \\ f_1(x) = a \cos(\varphi(x)) \end{cases}$$

Based on this map, group P can be related to I' group pixel values. The arbitrary pixel value is calculated in relation to a given gamma value.

Let $\gamma(x) = h(x)$, and the gamma correction function is defined as equation (4):

$$g(x) = 255 \left(\frac{x}{255} \right)^{1/\gamma(x)} \tag{4}$$

where $g(x)$ represents the output pixel correction value in grayscale.

Once this approach is applied, the correction value of a pixel will be connected to the value of the original pixel which satisfies the image correction requirements.

Image Segmentation

Background interference in CXR pictures may be efficiently suppressed by segmenting the ROI in the lungs (Li et al., 2019). The lung segmentation goal is to remove all unwanted background and retain the lung area. This process also aims to decrease noise that might interfere with model prediction. In this study, U-Net CNN, a semantic segmentation algorithm has been utilised for the image segmentation tasks as it outperforms the classic CNN architecture. The segmentation process extracted the ROI of lungs for normal and pneumonia CXRs. Instead of supplying the whole CXR image into the classification model for detection of pneumonia, a segmentation process was employed. The output of this lung contour was used in next step for feature extraction analysis.

U-Net CNN architecture as shown in Figure 2 is a fully convolutional network (FCN) consists of two basic components which are a contraction path on the left side, also known as an encoder and an expansion path on the right side also known as decoder whereby the contraction path has a function of recording image information, while expansion path utilizes the encoded information to provide segmentation output. In the middle between these two paths, the architecture consists of skip connections that concatenate the data and this concatenation of feature maps enables the U-Net model model to localize information in the semantic segmentation process.

Firstly, the segmentation process started with the contraction path also known as encoder down sampled the picture and captured the context by stacking the standard convolutional and max pooling layers. The contraction path was designed according to typical architecture of a convolutional network. The contraction path in the generated UNet model contains convolutional layers and the activation function that was used is the rectified linear unit (ReLU) activation function (Shaziya &

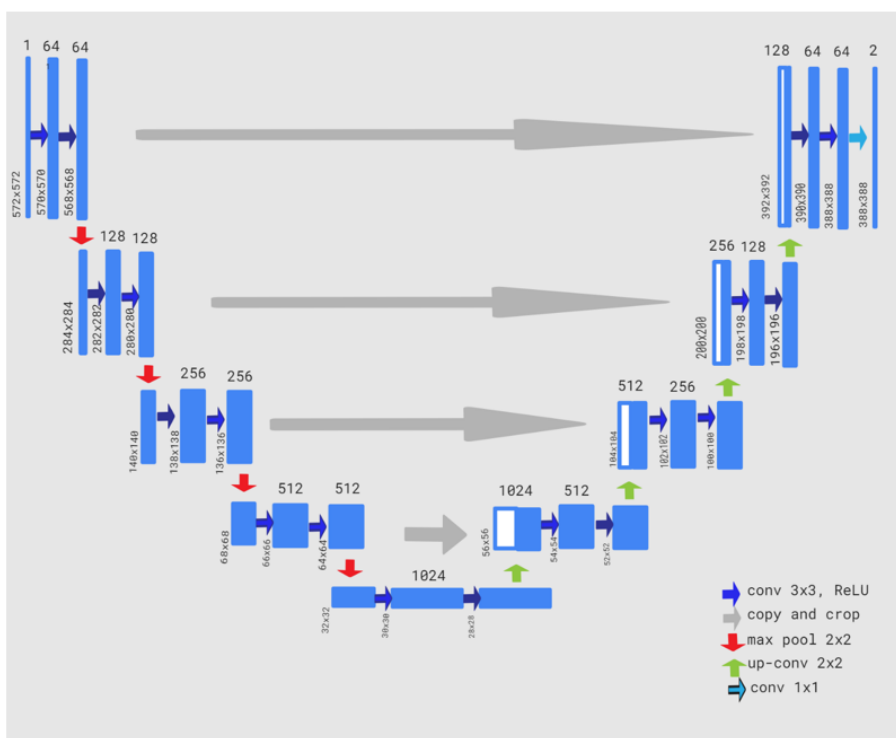


Fig. 2 CNN U-Net architecture (Ronneberger et al., 2015).

Shyamala, 2020). In the contraction path, on the top is where the process started by resizing the input image and went to the input layers. These input images passed through the convolutional layer of 3 by 3 matrix followed by the ReLU activation layer then produced the output of the first top level of contracting path. In the convolutional layer, there is a filter known as kernel that convolved with the input image and created an activation map. The ReLU activation layer as activation function allowed the model to learn complex functional mappings between the inputs and response variables. Next, the output image from the first level passed through the max pooling layer of stride 2. In the max pooling layer, the 2x2 matrix was employed. The maximum value of pixels was replaced in the 2 by 2 matrix. Max pooling layer helps reduce the spatial size of the convolved features and also helps reduce overfitting by reducing the dimension and complexity of the images. These processes were repeated until the images reached the lowest layer. Each encoding block composed of two 3x3 convolutional layers (unpadded convolutions) applied consecutively, each followed by a rectified linear unit (ReLU) and a 2x2 max pooling operation with stride 2 for downsampling. The number of feature channels was doubled at each downsampling step (Ronneberger et al., 2015).

The expanding path, or decoder path, on the other hand, is meant to generate the segmentation map utilising the extracted features and employs an up-sampling of the feature map concatenated with the cropped feature map from the contracting path (Kumarasinghe et al., 2022). Each block in the expansion route comprises of an upsampling of the feature maps followed by a 2x2 convolutional operation, a concatenated series of equivalent feature vectors from the contraction route, and two 3x3 convolution operations, each followed by activation function ReLU. At the conclusion, a 1x1 convolutional operation was used to map each 32-section feature map to two different classes (Kalane et al., 2021). The output after the 1 by 1

convolution layer at the expansive path is the output segmentation map that has two channels where one for foreground and one for the background class.

The backbone of the CNN is the convolutional layers, which entail a mathematical computation by convolving two separate functions, which in this case, the input images and a set of weights known as the kernel. This process results in a layer of feature maps. The convolutional layers are in charge of feature extraction, where it learned simple features like colour and edges in the first layer and more complicated information as the layer progresses.

Features Extraction

The lung contours obtained as segmented output from the previous segmentation process were used for the features extraction analysis. Many features were considered for the extraction purpose for the detection of pneumonia. Some of the features included are the visual, texture, intensity and geometric moment. Different analyses were carried out for different parameters of feature extraction (Goyal & Singh, 2021).

The lung area of the CXR can be considered as one of the vital features to classify the lung into normal or abnormal. The detection of lung areas is generally the initial step in the computerized analysis of chest radiography. The extent of the lungs allows the medical practitioners to conduct a more thorough assessment of the lungs' condition. The area is obtained by the summation of areas of pixels in the image that is registered as 1 in the binary image obtained as indicate in equation (5).

$$A = n\{1\} \quad (5)$$

where, $n\{ \}$ represents the count of numbers of the pattern within the curly brackets.

The area of the segmented lungs from the previous segmentation process is extracted for the feature extraction analysis by using MATLAB. The area of all images for both classes normal and pneumonia are extracted.

Performance Evaluation

The main purpose of this feature extraction analysis was to validate the reliability of the U-Net segmentation model to segment the lungs CXR. The result of the statistical analysis will validate whether both classes have different features. Therefore, it can prove the result of the segmentation whether accurate or not to differentiate between normal and pneumonia. Based on the area value, the study performed statistical analysis using t-test where it is a type of inferential statistic used to determine if there is a significant difference between the means and variance of two groups, which may be related in certain features.

Only the segmented images that produce the highest accuracy will be used for the feature extraction analysis in this study. In the statistical analysis, the mean, standard deviation and variances of all images in both classes were obtained to perform the t-test. From the t-test, the value of the t-stat was observed to classify between the normal and pneumonia classes. The hypothesis that can be made based on the t-stat value is the greater the difference between two sample sets, the greater the value of t-stat. Therefore, if there are differences in features between the normal and pneumonia segmented images, the value of the t-stat would be higher. If this result is obtained, it can indicate that the segmentation process is successful. The t-statistic measures how many standard errors the coefficient is away from zero. Generally, any t-value greater than +2 or less than - 2 is acceptable. The higher the t-value, the greater the confidence we have in the coefficient as a predictor. Low t-values are indications of low reliability of the predictive power of that coefficient.

$$t = \frac{(\bar{x}_1 - \bar{x}_2) - (\mu_1 - \mu_2)}{\sqrt{\frac{s_1^2}{n_1} + \frac{s_2^2}{n_2}}} \quad (6)$$

The null hypothesis (H0) and alternative hypothesis (H1) of the Independent Samples t Test can be expressed in two different but equivalent ways:

H0: $\mu_1 = \mu_2$ ("the two population means are equal")

H1: $\mu_1 \neq \mu_2$ ("the two population means are not equal")

OR

H0: $\mu_1 - \mu_2 = 0$ ("the difference between the two population means is equal to 0")

H1: $\mu_1 - \mu_2 \neq 0$ ("the difference between the two population means is not 0")

where μ_1 and μ_2 are the population means for group 1 and group 2, respectively.

The hypothesis that can be made on the t-score is the larger the t- score, the more difference exists between the groups while the smaller the t-score, the more similarity exists in the group.

RESULT AND DISCUSSION

Contrast Enhancement

The result obtained after applying the CLAHE contrast enhancement technique shows that there is a slight difference between original CXR and enhanced CXR while gamma-correction based technique, result shows that the enhanced CXR becomes darker. This enhancement process using CLAHE and gamma correction-based enhancement techniques unintentionally disrupts the important information of the CXR images for the detection of pneumonia. These are proved by the histogram obtained where the pixels in the original images is more equalised between the bright and dark region compared after applying the contrast enhancement. However, comparing between CLAHE and gamma correction-based enhancement, this study concludes that the output image and the histogram after applying CLAHE technique is the best in enhancing the CXR images. This can be observed further in the next step which is segmentation process. Therefore, this study concludes that not all CXR images are suitable to be applied contrast enhancement as the pre-processing steps.





Type of enhancement technique	Original CXR image	Output CXR image
CLAHE		
Gamma correction		

Fig 3. CXRs original image and after the contrast enhancement.

Image Segmentation

Based on the results obtained in Figure 4, the segmentation model for the normal class produced better segmented lungs compared to the pneumonia CXR images. This finding is supported by the accuracy value tabulated in Table 1 which were obtained for both CLAHE and Gamma enhanced CXR images segmented using the U-Net model.

the images after applying the CLAHE technique have features that is more obvious to differentiate the pneumonia with the background because the segmentation can segment the ROI of the lungs better compared to the CXR images without applying any enhancement process and images after applying gamma correction-based enhancement. As mentioned in Section 3.2xxx, the output images of CLAHE and the original images only shows slightly difference, however the segmentation model

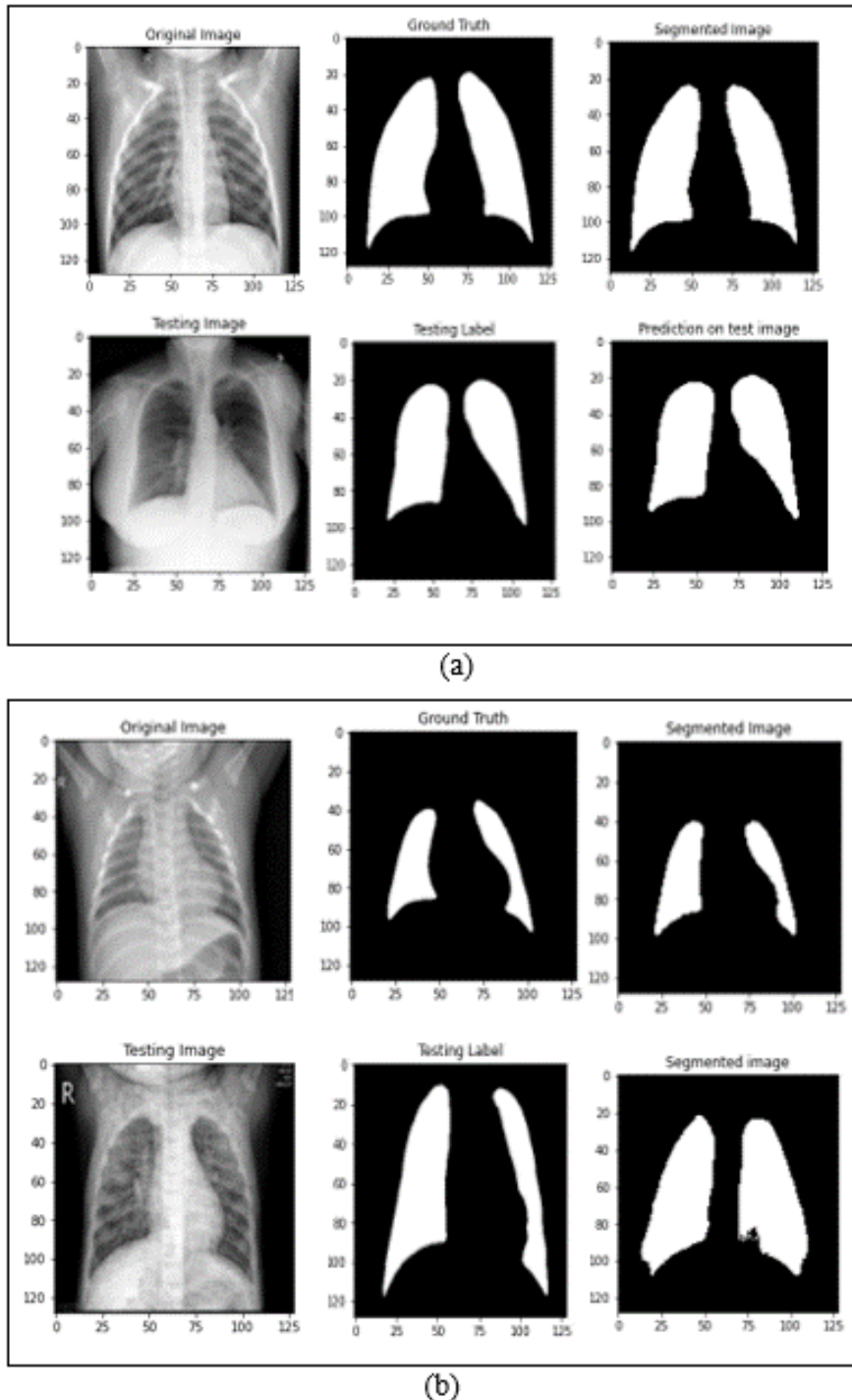


Fig. 4 (a) normal CXR and (b) pneumonia CXR before and after the seamentation process.

The accuracy of the U-Net CNN segmentation for the CLAHE obtained the highest value which are 0.9582 and 0.8798 for Normal and Pneumonia class respectively. The accuracy for the U-Net CNN segmentation of the images after applying the gamma-correction based enhancement obtain the low accuracy which are 0.9548 and 0.8621. Therefore, we can conclude that

developed proves that CLAHE enhanced images produce better segmentation output. As for the segmentation model with gamma-correction, the important information of the images of lungs were removed during enhancement process, thus producing a lower accuracy lung segmentation.

Table 1 Value for the accuracy of the U-Net segmentation models.

	Original	CLAHE	Gamma
Normal	0.9558	0.9582	0.9548
Pneumonia	0.8676	0.8798	0.8621

Feature Extraction Analysis

The analysis uses the segmented CXR image with CLAHE enhancement technique for both normal and pneumonia classes. The area of the segmented lungs was extracted from the output images for both classes. Statistical analysis using independent samples t-test was performed to differentiate between the two classes. The result shown in Table 2 validates the segmentation process by U-Net is accurate and reliable.

Table 2 Result of the statistical analysis for the features extraction

	Normal	Pneumonia
Mean	334.62	227.35
Variance	113793.90	2554.84
Observations	400	495
Pooled Variance	52188.41	
t Stat	6.98	
P(T<=t) one-tail	2.89	
t Critical one-tail	1.65	
P(T<=t) two-tail	5.78	
t Critical two-tail	1.96	

The result of the statistical analysis for the features extraction. From the area extracted, the study obtained the mean and variance for both classes and performed the test. From the result, the value obtained is 6.98 which is high and it can be concluded that there is difference between the normal and pneumonia segmented images.

CONCLUSION

As a conclusion, the U-Net CNN segmentation model developed for normal class has achieved 95.58%, 95.82% and 95.48% accuracy for original, CLAHE and gamma-correction based enhancement CXR images respectively. On the other hand, for pneumonia class, the performance of U-Net segmentation model has achieved 86.76%, 87.98% and 86.21% of accuracy for original, CLAHE and gamma-correction based enhancement CXR respectively. This finding suggested that U-Net CNN with CLAHE enhancement technique could be utilized for CXR images segmentation and can be highly useful for further intervention to facilitate medical practitioners in their decision-making in further processes.

ACKNOWLEDGEMENT

This Authors would like to express their gratitude to Universiti Teknologi Malaysia and the Ministry of Higher Education under Fundamental Research Grant Scheme (FRGS/1/2020/ICT02/UTM/02/4) for supporting this work.

REFERENCES

Apostolopoulos, I. D. and Mpesiana, T. A. 2020. COVID-19: Automatic detection from X-ray images utilizing transfer learning with Convolutional Neural Networks. *Physical and Engineering Sciences in Medicine*, 43(2), 635–640.

Dallal, A. H., Agarwal, C., Arbabshirani, M. R., Patel, A., Moore, G. 2017. Automatic estimation of heart boundaries and cardiothoracic ratio from chest x-ray images. In *Medical Imaging 2017: Computer-Aided Diagnosis*. SPIE, 10134, 134-143.

Goyal, S. and Singh, R. 2021. Detection and classification of lung diseases for pneumonia and covid-19 using machine and Deep Learning Techniques. *Journal of Ambient Intelligence and Humanized Computing*, 1-21.

Jahangard, S., Zangoeei, M. H., Shahedi, M. 2020. U-net based architecture for an improved multiresolution segmentation in medical images. *arXiv preprint arXiv 2007.08238*.

Lie, J., Lysaker, M., Tai X. C. 2006. A binary level set model and some application to Mumford–Shah image segmentation. *IEEE Transaction on Image Processing* 15, 1171–1181.

Kalane, P., Patil, S., Patil, B. P., Sharma, D. P. 2021. Automatic detection of covid-19 disease using U-net architecture based fully convolutional network. *Biomedical Signal Processing and Control* 67, 102518.

Koonsanit, K., Thongvigitmanee, S., Pongnapang, N., Thajchayapong, P. 2017. Image enhancement on digital X-ray images using N-clahe. 2017 10th Biomedical Engineering International Conference (BMEiCON).

Kumarasinghe, H., Kolonne, S., Fernando, C., Meedeniya, D. 2022. U-Net based chest X-ray segmentation with ensemble classification for covid-19 and pneumonia. *International Journal of Online and Biomedical Engineering (IJOE)* 18(07), 161–175.

Kundu, R., Das, R., Geem, Z. W., Han, G. T., Sarkar, R. 2021. Pneumonia detection in chest X-ray images using an ensemble of Deep Learning Models. *PLOS ONE* 16(9), e0256630.

Lal, S., Rehman, S. U., Shah, J. H., Meraj, T., Rauf, H. T., Damaševičius, R., Mohammed, M. A., Abdulkareem, K. H. 2021. Adversarial attack and defence through adversarial training and feature fusion for diabetic retinopathy recognition. *Sensors* 21(11), 3922.

Li, B., Kang, G., Cheng, K., & Zhang, N. 2019. Attention-guided convolutional neural network for detecting pneumonia on chest x-rays. 41st Annual International Conference of the IEEE Engineering in Medicine and Biology Society (EMBC).

Mazzone, P. J., Obuchowski, N., Phillips, M., Risius, B., Bazerbashi, B., Meziane, M. 2013. Lung cancer screening with Computer Aided Detection Chest Radiography: Design and results of a randomized, controlled trial. *PLoS ONE* 8(3), e59650.

Mique, E. and Malicdem, A. 2020. Deep residual U-net based lung image segmentation for lung disease detection. *IOP Conference Series: Materials Science and Engineering* 803(1), 012004.

Mittal, A., Hooda, R., Sofat, S. 2017. Lung Field Segmentation in chest radiographs: A historical review, current status, and expectations from Deep Learning. *IET Image Processing* 11(11), 937–952.

Nirmala Devi, S.; Kumaravel, N. (2008). Comparison of active contour models for image segmentation in X-ray coronary angiogram images. *Journal of Medical Engineering and Technology* 32(5), 408–418.

Qin, C., Yao, D., Shi, Y., Song, Z. 2018. Computer-aided detection in chest radiography based on Artificial Intelligence: A survey. *BioMedical Engineering OnLine*, 17(1), 1-23.

- Ramudu, K., Reddy, G. R., Srinivas, A., Krishna, T. R. 2013. Global region based segmentation of satellite and medical imagery with active contours and level set evolution on noisy images. *International Journal of Applied Physics and Mathematics*, 2(6), 449–453.
- Rauf, H. T., Lali, M. I., Khan, M. A., Kadry, S., Alolaiyan, H., Razaq, A., Irfan, R. 2021. Time series forecasting of COVID-19 transmission in Asia Pacific countries using Deep Neural Networks. *Personal and Ubiquitous Computing*, 1-18.
- Ronneberger, O., Fischer, P., Brox, T. 2015. U-Net: Convolutional Networks for Biomedical Image Segmentation. In Navab, N., Hornegger, J., Wells, W., Frangi, A. (eds) *Medical Image Computing and Computer-Assisted Intervention – MICCAI 2015*. MICCAI 2015. Lecture Notes in Computer Science (9351). Springer, Cham 234–241.
- Shaziya, H. and Shyamala, K. 2020. Pulmonary CT images segmentation using CNN and UNET models of Deep Learning. 2020 IEEE Pune Section International Conference (PuneCon).
- Souza, J. C., Bandeira Diniz, J. O., Ferreira, J. L., França da Silva, G. L., Corrêa Silva, A., de Paiva, A. C. 2019. An automatic method for lung segmentation and reconstruction in chest X-ray using Deep Neural Networks. *Computer Methods and Programs in Biomedicine*, 177, 285–296.
- Stolajescu-Crisan, C. and Holban, S. 2013. A comparison of X-ray image segmentation techniques. *Advances in Electrical and Computer Engineering*, 13(3), 85–92.
- Stolajescu-Crisan, C., Holban, S. 2014. An Interactive X-Ray Image Segmentation Technique for Bone Extraction. *Proceeding IWBBIO 2014*, 1164-1171.
- Teixeira, L. O., Pereira, R. M., Bertolini, D., Oliveira, L. S., Nanni, L., Cavalcanti, G. D., Costa, Y. M. 2021. Impact of lung segmentation on the diagnosis and explanation of covid-19 in chest X-ray images. *Sensors* 21(21), 7116.
- Wang, X., Peng, Y., Lu, L., Lu, Z., Bagheri, M., Summers, R. M. 2017. Chestx-Ray8: Hospital-scale chest X-ray database and benchmarks on weakly-supervised classification and localization of common thorax diseases. 2017 IEEE Conference on Computer Vision and Pattern Recognition (CVPR) 7.
- Xu, C. and Prince, J. L. 1998. Generalized gradient vector flow external forces for active contours. *Signal Processing* 71(2), 131–139.
- Yu, M., Xu, D., Lan, L., Tu, M., Liao, R., Cai, S., Cao, Y., Xu, L., Liao, M., Zhang, X., Xiao, S.-Y., Li, Y., Xu, H. 2020. Thin-section chest CT imaging of covid-19 pneumonia: A comparison between patients with mild and severe disease. *Radiology: Cardiothoracic Imaging* 2(2), e200126.
- Zimmerman, J. B., Pizer, S. M., Staab, E. V., Perry, J. R., McCartney, W., Brenton, B. C. 1988. An evaluation of the effectiveness of adaptive histogram equalization for contrast enhancement. *IEEE Transactions on Medical Imaging* 7(4), 304–312.